NUMERICAL ANALYSIS ON HEAT TRANSFER AND FLOW RESISTANCE PERFORMANCES OF A HEAT EXCHANGER WITH NOVEL PERFORATED WAVY FINS

Xuexi WANG*, Feng LIN

* Suzhou Chien-shiung Institute of Technology, Suzhou, 215411, China.

* Xuexi WANG; E-mail: xxwang_1@hotmail.com

In this paper, the experimental and numerical study of thermo-hydraulic characteristics of perforated wavy fin heat exchanger and unperforated wavy fin heat exchanger were conducted. Firstly, the two kinds of fins were studied under different air inlet velocity and constant inlet temperature. The results show that Nusselt number increases with Reynolds number and friction factor decreases with Reynolds number. Then, the performance of the two kinds of fins is numerically analyzed, and the simulation results are in good agreement with the experimental data. On this basis, the influence of different perforated fin parameters (fin height H, fin pitch s, wave amplitude wa, perforation number n, perforation diameter d) on the thermal performance of wavy fin heat exchanger is discussed. It is indicated that friction factor and Nusselt number increase with increasing aperture, wave amplitude, fin pitch and perforation number or decreasing fin height under constant Reynolds number condition. Finally, the performance evaluation of heat exchangers with different parameters is carried out to obtain the best performance heat exchanger parameters, which can provide a reference for the design of the new wavy fin heat exchanger.

Key words: *thermo-hydraulic performance, fin-plate heat exchanger, perforated, wavy fins, empirical correlations*

1. Introduction

The production process of the steel industry is often accompanied by high-temperature by-products, such as blast furnace slag, high-temperature exhaust gas and so on. These high-temperature by-products are directly discharged not only pollute the environment, but also waste a lot of high-quality heat [1, 2]. Therefore, if this part of the waste heat is effectively recovered, it is of great significance to energy saving, environmental protection and economic benefits [3, 4].At present, the mainstream core equipment in the field of industrial waste heat recovery is heat pipe heat exchanger, plate-fin heat exchanger(PFHE), and shell-and-tube heat exchanger. PFHE has attracted people's attention for its high heat transfer coefficient and compact structure in the past 30 years

For the fluidity and heat transfer of the PFHE, some scholars conducted the following research on the fin structure of the PFHE. Karthik et al. [5] experimentally analyzed the heat transfer characteristics of the louver fin heat exchanger used as an internal combustion engine radiator. Li et al. [6] analyzed the comprehensive performance of the serrated fin PFHE under low temperature conditions. Khoshvaght-Aliabadi et al. [7] conducted an experimental comparison about seven common channels of PFHEs based on energy evaluation standards. The results show that the vortex

channel has the best heat transfer coefficient, and the wavy channel shows the best performance at low Reynolds number. Gao et al. [8] Designed stainless steel wavy fins with plate-fin structure, and optimized structural parameters, including wavy Angle, wavy pitch and fin length, proposed a 3-D simulation model and experiment. Khoshvaght-Aliabadi et al. [9] experimentally studied the effect of delta winglets on the performance of PFHEs wave-shaped fins using Al_2O_3/water nanofluid as the flow medium. Wen et al. [10] comprehensively studied the heat transfer, flow resistance and stress distribution of sine wave fins based on fluid-structure coupling analysis, and proposed an improved structure of wave fins. Patrick Haider et al. [11] proposed a novel model for transient simulation of low-temperature PFHEs to calculate the heat transfer and pressure drop that occur during fluid flow of various fin types.Based on the research of the flow and heat transfer performance of the PFHE, scholars have carried out the following research on the optimization of the PFHE. Reneaume and Niclout [12], Pingaud [13] proposed MINLP optimization of PFHEs. Picon-Nunez et al. [14] proposed a design method for a compact PFHE designed to make full use of the pressure drop, and also proposed a simple surface selection based on volumetric performance index (VPI) method. Mishra et al. [15] proposed a cross-flow PFHE thermal economic design optimization based on genetic algorithm. Peng and Ling et al. [16] used back-propagation neural network (BP) and genetic algorithm (GA) to successfully apply to the optimal design of PFHE for the first time, and calculated the minimum weight and annual total of the heat exchanger cost.

In recent years, a large number of scholars have conducted research about PFHE with various fin structures. This article will further explore on the basis of wavy fin heat exchangers studied by predecessors. The heat transfer and flow characteristics of the wavy fin heat exchanger have been obtained by the wind tunnel experiment system. On this basis, experimental study and numerical simulation of perforated and unperforated wavy fin heat exchangers are carried out. First, the *Nu* and *f* of the two kinds of fins have been obtained by experiment, and compared with the simulation results, which verified the reliability and feasibility of the numerical simulation. Secondly, the effects of fin height, fin pitch, wave amplitude, perforation number and perforation diameter on Nusselt number (*Nu*) and friction factor (*f*) are studied. The comprehensive performance factor (η) of the fin is measured by $Nu/f^{1/3}$.

2. Experiment

2.1. New type of fin-plate heat exchanger

In this paper, a new type of perforated wavy fin heat exchanger (PWFHE) is proposed. The schematic diagrams of fin-plate structure are shown in Fig. 1. A single unit of PWFHE consists of fins and two clapboards. In the present work, perforated wavy fins are applied in the PWFHE. Fin parameters include fin height, H, fin pitch, s, fin thickness, δ, fin length, L, amplitude, A, wavelength, λ, perforation diameter, d and perforation number, n (n is the number of perforations in a single peak area). To further characterize the effect of amplitude and wavelength on fin performance, a dimensionless constant wave amplitude (wa) is introduced, which is defined as follows:

$$wa = 2A / \lambda \tag{1}$$

The purpose of this study is to investigate the effect of the fin structure on the thermo-hydraulic performance of the outside flow channel of a PWFHE. Twelve types of perforated wavy fin with different geometric parameters are proposed for the experimental tests and numerical simulations, as listed in Table 1.

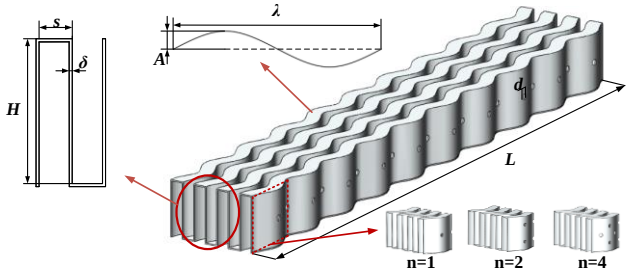

Fig. 1 Schematic diagrams of perforated wavy fin structure

Tab. 1 Parameters of wavy fin

Sample	H (mm)	s (mm)	δ (mm)	L (mm)	A (mm)	λ(mm)	Wa	d(mm)	n
1	9.5	2.2	0.2	105	0.9	10.5	0.171	/	/
2	7.5	2.2			0.9	10.5	0.171	1	1
3	11.5	2.2			0.9	10.5	0.171	1	1
4	9.5	1.4			0.9	10.5	0.171	1	1
5	9.5	3.0			0.9	10.5	0.171	1	1
6	9.5	2.2			1.2	12.5	0.192	1	1
7	9.5	2.2			1.4	13.5	0.207	1	1
8	9.5	2.2			0.9	10.5	0.171	1	1
9	9.5	2.2			0.9	10.5	0.171	2	1
10	9.5	2.2			0.9	10.5	0.171	3	1
11	9.5	2.2			0.9	10.5	0.171	1	2
12	9.5	2.2			0.9	10.5	0.171	1	4

2.2. Experimental apparatus

The experimental setup is composed of test section, air channel, temperature control system, steam-water cycle and a data acquisition system, as shown in Fig. 2. The low-pressure air in the air duct is inhaled by the centrifugal fan and discharged along the exhaust outlet. It flows through the fast section, the heating section and the stable section, and enters the test area after reaching the experimental conditions. The temperature control system can adjust the heating rate of the heating section by adjusting the throttle valve on the high-temperature saturated steam channel and changing the steam flow, and the temperature error is within ±0.5K. The gas-water heat cycle of this experiment adopts electric heating steam boiler to make the condensed water in the boiler heat up and evaporate to form high temperature saturated steam. After the air is heated, it is cooled by the condenser to become condensed water and then circulated back to the steam boiler. The temperature of inlet and outlet can be obtained by the above temperature control system, and the temperature of the fin can be obtained by the thermocouple on the Fin. The precision of the pre-calibrated thermocouple is 0.5 K. The pressure drop on the fins is measured by the calibrated differential pressure transmitter DR1200. The measurement range is 0-1.5kPa and the measurement accuracy is 0.05%. After all data is integrated through the PC port, further data processing can be done. In order to ensure the reliability of the experimental data, it is necessary to analyze the relative uncertainty of the experimental results. Finally, the relative errors of Nu and f are 4.22% and 2.15%, respectively.

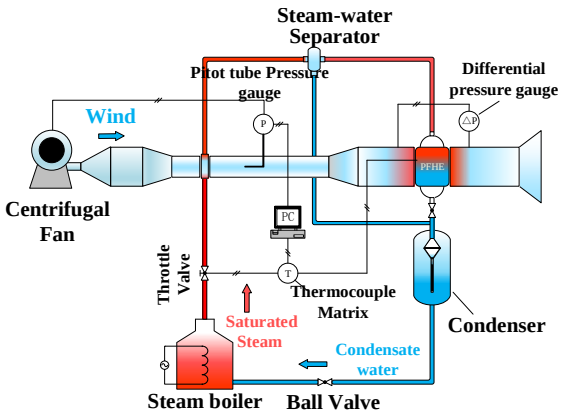

Main instruments and equipment for experiments

Instrument	Model	Function
Common thermocouple	Self-made, Copper constantan T-type, diameter Φ0.5mm	Measure outlet air temperature
Sheathed thermocouple	WREK, Outer diameter of casing Φ3mm	Measure inlet air temperature
Micro manometer	MP200	Measure the flow pressure drop of the wind tunnel system
Pitot	L-Φ2mm	Measure the speed of air in the wind tunnel system
Temperature acquisition system	NI4350	Analyze and collect thermocouple temperature data
High precision multimeter	UT70D	Measuring resistance wire resistance and voltage

Fig. 2 Schematic diagram of experimental apparatus (left) , instruments introduction (right)

2.3. Experimental procedures

The experimental conditions are set as: Range of Reynolds number (*Re*) is 1500~7000, Inlet temperature is 27°C, Pressure at the steam inlet is 0.12 MPa. The average value of several actual measured values is taken under the same conditions. By comparing the heat balance error between the air side and the steam side, the data whose error less than 4% is imported into the calculation, and data above this value is discarded. Heat transfer at the steam side and at the air side is calculated using the follow equations, respectively:

$$Q_v = m_v h_v, \quad Q_a = m_a c_{pa} \Delta T_a \tag{2}$$

Where Q is heat transfer rate, kW, m is mass flow rate, kg/s, h is enthalpy, kJ/kg, c_p is specific heat, kJ/kg·K, ΔT is temperature difference, K, and the subscript v means vapour, a means air。

3. Numerical simulations

3.1. Model

Because the overall structure of the PWFHE is cyclic and symmetric, the heat transfer and flow performance of the integral PWFHE can be reflected by establishing a unit flow channel.

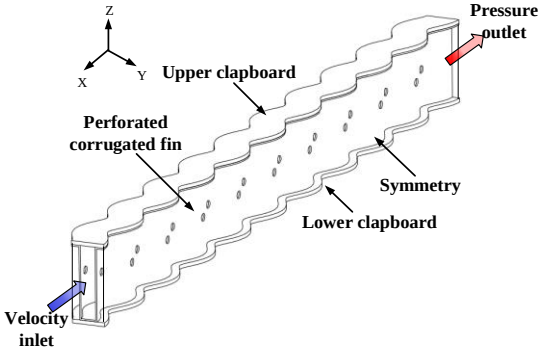

Fig. 3 Three-dimensional model of perforated wavy fin flow channel

As shown in Fig. 3, the three-dimensional model of a single flow channel of the PWFHE consists of upper and lower clapboards and perforated wavy fins. In order to study the influence of different geometric parameters on the thermo-hydraulic performance of PWFHE, 12 sets of fin parameters were used to numerically simulate the thermo-hydraulic performance of the PWFHE, as listed in Table 1.

3.2. Governing equations

To simplify numerical calculations, the following assumptions are made: the air flow is three-dimensional, stable, incompressible and qualitative. The effects of thermal radiation, natural convection, viscous energy diffusion and gravity are ignored. During the experiment, *Re* of the perforated wavy fin channel is in the turbulence range. Therefore, the standard *k-ε* model is adopted. Ignoring the influence of volume force, the corresponding fluid domain continuity equation, momentum equation and energy equation are as follows:

(1) Continuity equation

$$\frac{\partial(\rho u_i)}{\partial x_i} = 0 \tag{3}$$

(2) Momentum equations (*k-ε* model)

$$\frac{\partial}{\partial x_i}(\rho k u_i) = \frac{\partial}{\partial x_j}\left[\left(\mu + \frac{\mu_t}{\sigma_k}\right)\frac{\partial k}{\partial x_j}\right] + \eta_t \frac{\partial u_i}{\partial x_j}\left(\frac{\partial u_i}{\partial x_j} + \frac{\partial u_j}{\partial x_i}\right) - \rho\varepsilon \tag{4}$$

$$\frac{\partial}{\partial x_i}(\rho \varepsilon u_i) = \frac{\partial}{\partial x_j}\left[\left(\mu + \frac{\mu_t}{\sigma_\varepsilon}\right)\frac{\partial \varepsilon}{\partial x_j}\right] + c_1 \frac{\varepsilon}{k}\eta_t \frac{\partial u_i}{\partial x_j}\left(\frac{\partial u_i}{\partial x_j} + \frac{\partial u_j}{\partial x_i}\right) - c_2 \rho \frac{\varepsilon^2}{k} \tag{5}$$

(3) Energy equation

$$\frac{\partial(\rho u_i T)}{\partial x_i} = \frac{\lambda}{c_p}\frac{\partial^2 T}{\partial x_i^2} \tag{6}$$

where, $c_1 = 1.44$, $c_2 = 1.92$, $\sigma_k = 1.0$, $\sigma_\varepsilon = 1.3$, $c_\mu = 0.09$, $\mu_t = c_\mu \rho k^2 / \varepsilon$.

3.3. Mesh

The grid of the calculation model is generated by ICEM, and is divided by an unstructured tetrahedral grid, as shown in Fig. 4. Since the fluid flow boundary layer and thermal boundary are close to the wall, the mesh of fin area is refined to ensure the accuracy and reduce errors of numerical simulation. Before exporting the grid, to improve the quality of the mesh, further adjustment to the grids is performed. To ensure that the calculation result is independent of the grids number, the *Nu* is validated for grid independence, and more details is presented in section 5.2.1.

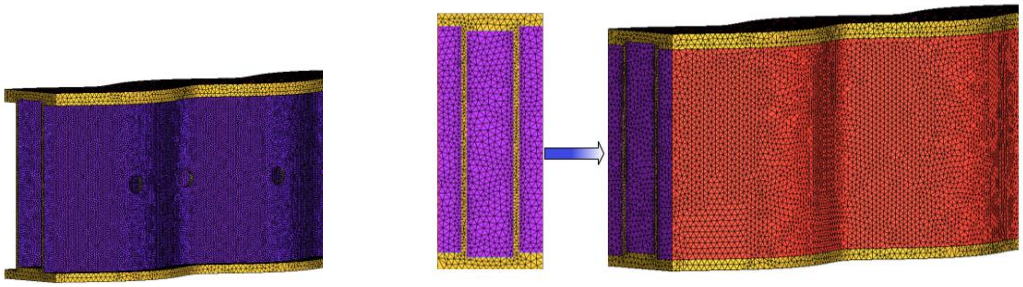

Fig. 4 Schematic diagrams of perforated wavy fin grid (left) and overall grid (right)

3.4. Boundary conditions and computational approach

In the numerical simulation of the perforated wavy fin channel, the fluid inlet is based on the velocity inlet condition, and the inlet temperature is 300K.In order to ensure the rapid convergence of the calculation when the fluid reflux occurs, the fluid outlet boundary condition is set to the pressure outlet (constant pressure).The outer surface of the upper and lower partitions is set as a constant wall temperature boundary condition, the temperature is 373.15K. Besides, the solid material is aluminium,.the fluid material is air. And the physical properties are shown in Table 2.

Tab. 2 Physical properties of solid and fluid

Material	Density(kg/m^3)	Specific heat(J/(kg·K)	Thermal conductivity(W(m·K))	Viscosity(Pa·s)
Solid: aluminum	2719	871	202.4	-
Fluid: air	1.225	1006.43	0.0242	1.789×10^{-5}

3.5. Numerical solution method

In current work, numerical simulation is performed by the commercial computational fluid dynamics software ANSYS FLUENT 18.0. The computer machine with i5 CPU and 16 cores is used and computional time of each case is about one hour. In this study, the pressure-velocity coupling is based on the SIMPLE algorithm. The discrete format of the momentum equation and the energy equation are using a second-order upwind formulation. The condition of convergence is that the calculation residual of the energy equation to be less than 10^{-8}, the calculation residual of other equations is less than 10^{-4}. If the residual is less than the threshold and does not change significantly with further iteration, then the calculation is considered as converged.

4. Data reduction

To evaluate the performance of PWFHE and UPWFHE, the following parameters are defined.

The hydraulic diameter D_e and Reynolds number Re are defined as:

$$D_e = \frac{4\times(s-\delta)\times H}{2\times[(s-\delta)+H]} \tag{7}$$

$$Re = \frac{\rho u D_e}{\mu} \tag{8}$$

Where ρ is density, kg/m^3, u is velocity of inlet, m/s, and μ is viscosity, Pa·s.

The Nusselt number Nu is calculated by the following equation:

$$Nu = \frac{qD_e}{\lambda(T_w - \frac{T_{in}+T_{out}}{2})} \tag{9}$$

$$q = \frac{Q}{A} \tag{10}$$

λ is Thermal conductivity, kW/m·K, T_{in},T_{out} and T_w are inlet temperature, outlet temperature and wall temperature respectively, ℃, q is heat flux density, kW/m^2, A is heat exchange area, m^2.

The coefficient of friction f is defined as:

$$f = \Delta P \frac{D_e}{4L} \frac{2}{\rho u^2} \tag{11}$$

ΔP is the pressure drop, Pa , and L are fin length, mm.

5. Results and discussion

5.1. Experimental results

In this study, in order to verify the reliability of the test, samples 1 and 8 were tested repeatedly. Set the fluid inlet according to the working conditions, the inlet temperature is 300K, and the steam inlet pressure is maintained at 0.12MPa.

On the air side, measure the outlet temperature and outlet pressure at six different *Re*. The four experimental calculation results of the two sample heat exchangers are shown in Fig. 5. As *Re*

increases, *f* decreases and *Nu* increases. The *Nu* and *f* of the perforated wavy fin heat exchanger are larger than those of the unperforated wavy fin heat exchanger. Obviously, the perforation allows the fin to obtain better heat transfer performance, but increases the pressure drop. The two experimental results of the same type of heat exchanger are similar, which ensures the reliability of the experimental data.

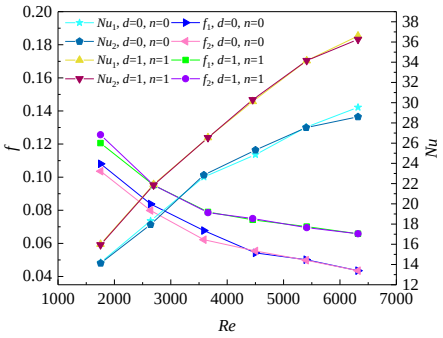

Fig. 5 Reliability tests: *f* and *Nu* vs. *Re*

5.2. Numerical simulation

5.2.1 Grid independence and model validation

In order to reduce the simulation error, it is necessary to verify the independence of the grid.The calculated *Nu* values of the same model with different mesh numbers are shown in Fig. 6. Finally, the grid number of UPWFHE is 2.2 million, and the grid number of PWFHE is 2.85 million.

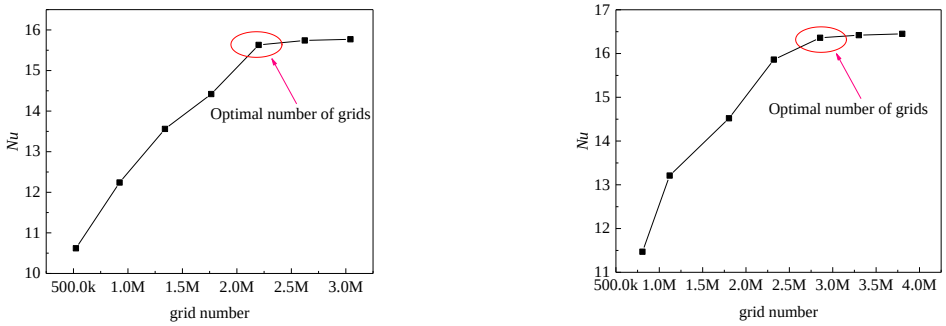

Fig. 6 grid numbers of unperforated(left) and perforated(right)

The *f-Re* and *Nu-Re* curves of the PWFHE and UPWFHE are obtained by numerical simulation of the two samples at different air inlet speeds. As shown in Fig. 7, the results show that the simulation results are in good agreement with the experimental results, and the error of the results obtained by the two samples is within 20%, which verifies the validity of the numerical simulation. The main reason for the error is that the influence of temperature on physical parameters is ignored.

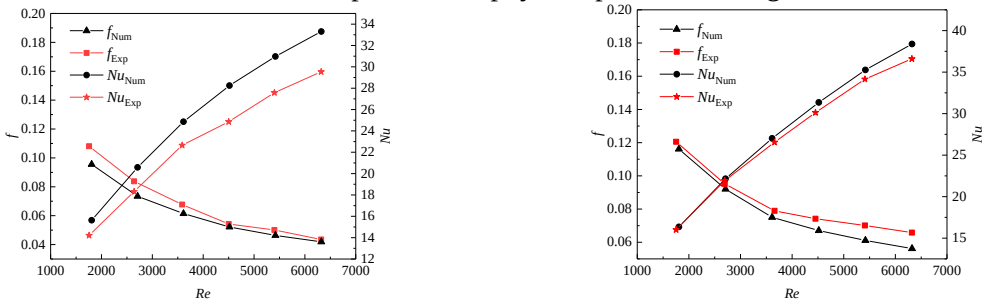

Fig. 7 Numerical and experimental comparison of UPWFHE(left) and PWFHE(right)

5.2.2 Temperature distribution

Two types of heat exchangers, sample 1 (unperforated wavy fin) and sample 8 (perforated wavy fin) are analyzed for temperature field. The inlet speed is 5m/s, inlet temperature is 300K, the temperature of clapboard is 373.15K, and the entire length of the chanel is 105mm.

Fig. 8 shows the temperature field distribution of UPWFHE and PWFHE in two directions. Obviously, the thermal conductivity of air is much smaller than aluminum, thus demonstrating an apparent temperature gradient. And there is no fin to enhance heat transfer in the center of the channel, the temperature is lower and the change is small.The comparison of the two figures shows that PWFHE and UPWFHE have similar temperature distributions and changing trends. However, due to the perforation in the middle of the PWFHE fins, the thermal boundary layer is destroyed and the degree of agitation between the fluids is enhanced. Therefore, the heat transfer between the central part and both sides of the channel and the fin is enhanced, so the temperature of the central part and both sides is higher than that of the unperforated wavy fins.

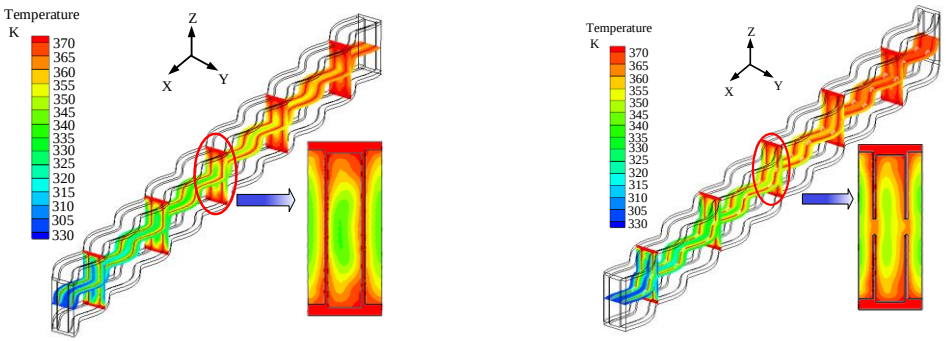

Fig. 8 Temperature distributions of unperforated (left) and perforated (right)

5.2.3 Effect of geometric parameters

(1) Effect of the fin height

The relationship between *Nu* and *f* with *Re* changes is shown in Fig. 9. It can be seen from the figure that at the constant *H*, *f* decreases but *Nu* increase with the increase of *Re*. When *Re* is constant, both *Nu* and *f* decrease as *H* increases, the *Nu* and *f* with *H*=7.5mm is 12.4%~17.6% and 20.0%~28.6% larger than that with *H*=11.5mm. For fin channels with the same *H* and *Re*, perforated fin channels have larger *f* and *Nu* than unperforated fin channels. The decrease in pressure drop has a negative effect on *f* . It can be clearly seen that increasing the height of the fin will reduce the temperature difference, and according to equation (10), the heat flux density of the air will also decrease. Finally, *Nu* decreases as the height of the fin increases, which means that the heat flux density of the air is much larger than the temperature difference.

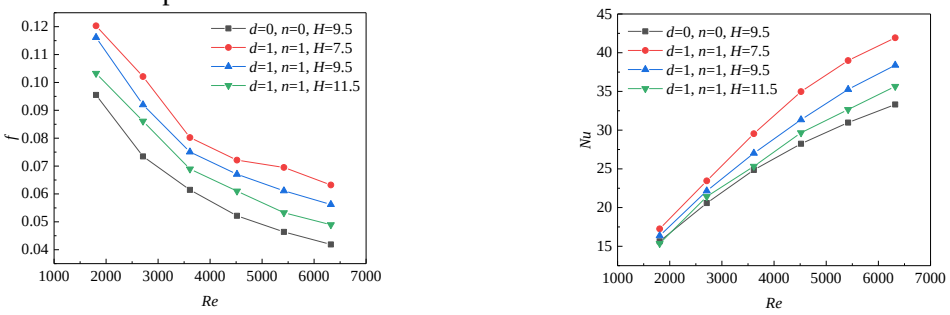

Fig. 9 Effect of fin height (*H*) on *f* (left) and *Nu*(right)

(2) Effect of fin pitch

Fig. 10 shows the relationship between *Nu* and *f* as *Re* changes under unperforated wavy fin channels (sample 1) and perforated wavy fin channels with different fin pitch (samples 4, 5 and 8). It can be seen from the graph that in the case of constant fin pitch, f decreases but *Nu* increases with the increase of *Re*. In the case of constant *Re*, with the increase of fin pitch, both *Nu* and *f* increase, the *Nu* and *f* with *s*=3.0mm is 12.6%~18.9% and 32.6%~45.4% larger than that with *s*=1.4mm. For two fin channels with the same fin pitch under the same *Re*, the perforated wavy fin channel has larger *f* and *Nu* than the unperforated wavy fin channel. The results show that with the increase of the fin pitch, the hydraulic diameter increases, but the flow resistance, pressure drop and flow velocity decrease, and the degree of flow velocity decrease is much greater than the pressure drop, therefore, *f* appears to increase with the increase of the fin pitch. The increase in hydraulic diameter expands the primary surface area and enhances heat transfer, resulting in an increase in *Nu*. At the same time, the increase of *Re* will further increase the positive correlation between fin pitch and *Nu*.

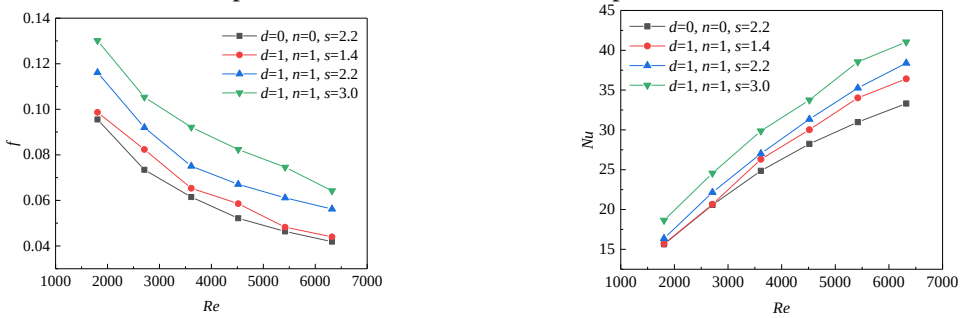

Fig. 10 Effect of fin pitch (*s*) on *f* (left) and *Nu*(right)

(3) Effect of wave amplitude

The variations of *Nu* and *f* via *Re* at different wave amplitude (*wa*) of perforated wavy fin channels (Samples 6, 7 and 8) and unperforated (Sample 1) are illustrated in Fig. 11. It can be seen from the figure that at a constant *wa*, *f* decreases but *Nu* increases as *Re* increases. At a constant *Re*, *Nu* and *f* both decrease as the *wa* increases, the *Nu* and *f* with *wa*=0.21mm is 6.7%~15.2% and 13.8%~25% larger than that with *wa*=0.17mm. Results show that, with the increase of wa, the geometric characteristics of the wavy structure become more obvious and the agitation on the fluid is stronger, leading to larger *Nu*, pressure drop and *f*. It is noteworthy that as wa increase, the growth rate of *f* is much greater than that of *Nu*, and the lifting space of *Nu* will be smaller. This is because when wa rises to a certain extent, the vortex and flow dead zone will be formed in the wave trough, which leads to the insufficient agitation of the wavy structure to the main flow region, and the improvement of heat transfer performance is not obvious.

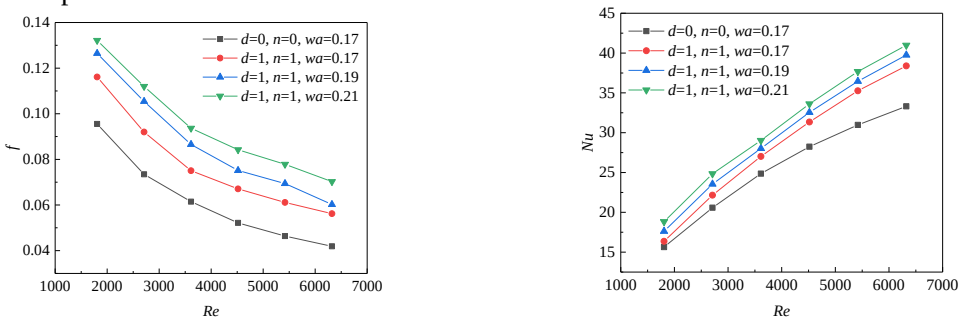

Fig. 11 Effect of wave amplitude (*wa*) on *f* (left) and *Nu*(right)

(4) Effect of perforation number

Fig. 12 depicts the comparison of *Nu* and *f* between different perforation number of perforated wavy fin channels (Samples 8, 9 and 10) and unperforated wavy fin channel (Sample 1). It is obvious that when perforation number is constant, *f* decreases but *Nu* increases as *Re* increases. At a constant *Re*, as growth of perforation number, both flow resistance and pressure drop increase, resulted a larger *f*, the *Nu* and *f* with *n*=4 is 5.4%~55% and 8.9%~17.8% larger than that with *n*=1. Meanwhile, the increase of perforation number will reduce the heat transfer area, increase the agitation of the fluid, destroy the thermal boundary layer, and make the fluid temperature more uniform in the channel. However, the increase of the agitation is greater than the loss of heat transfer area, so *Nu* increases with the increase of perforation number.

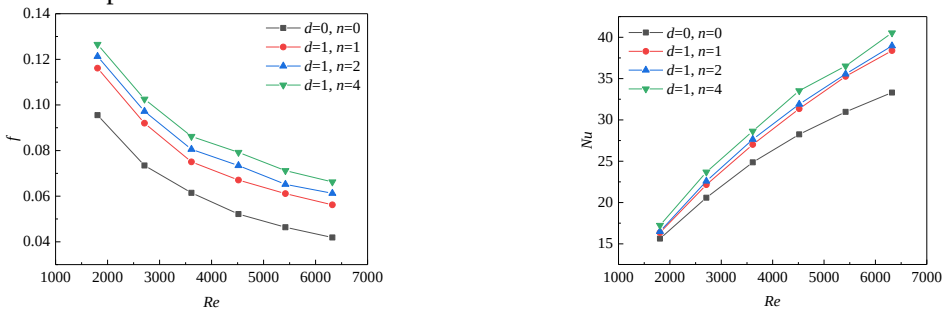

Fig. 12 Effect of number of perforations (*n*) on *f* (left) and *Nu*(right)

(5) Effect of perforation diameter

The variation of f and *Nu* versus *Re* number for various perforation diameter of perforated wavy fin channels (Samples 8, 11 and 12) and unperforated wavy fin channel (Sample 1) is shown in Fig. 13. It can be noticed that with perforation diameter being constant, *f* decreases but *Nu* increases as *Re* increases. When *Re* is the same, both *f* and *Nu* augment with the growth of perforation diameter, the *Nu* and *f* with *d*=3mm is 4.5%~10.8% and 13.8%~23.2% larger than that with *d*=1mm. Evidently, increasing the perforation diameter will reduce the heat transfer area of the fin channel; increase the flow resistance and the degree of fluid agitation. It is worth noting that with the increase of perforation diameter, the growth of fluid agitation and the destruction of thermal boundary layer are greater than the loss of heat transfer area, so *Nu* increases with the increase of perforation diameter.

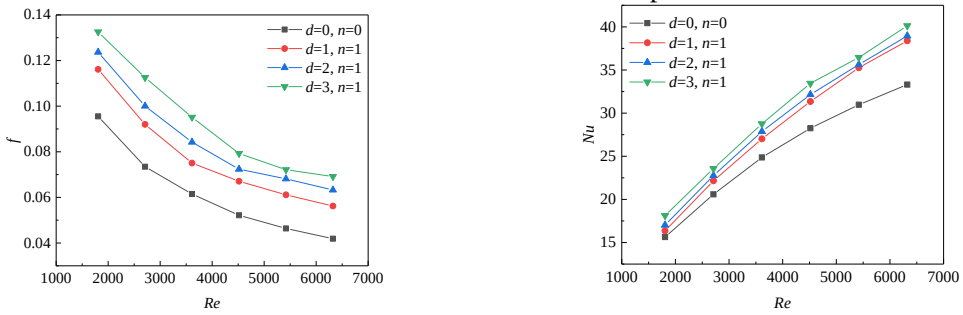

Fig. 13 Effect of perforation diameter (*d*) on *f* (left) and *Nu*(right)

5.3. performance analysis of these fins

The principle of heat exchanger design is to obtain higher heat transfer efficiency at the expense of smaller flow resistance. Therefore, in this paper, the comprehensive performance factor (η) of wavy fin heat exchanger is introduced, which is defined as follows:

$$\eta = \frac{Nu}{f^{1/3}} \tag{12}$$

The larger the η of fins, the better the heat transfer performance. The variation of η via *Re* for perforated wavy channels (Sample 2, 3, 4, 5, 6, 7, 8, 9, 10, 11, 12) and unperforated wavy channel (Sample 1) are shown in Fig. 14. With a constant *Re*, it should be noted that at low Reynolds numbers (*Re*=2000~3000), the η of perforated wavy fin channel with different fin parameters does not increase significantly compared to the unperforated wavy fin channel. When the range of *Re* is 3500~6500, it is evident that η of other perforated wavy fin channels are greater than that of unperforated wavy fin channels. Among them, the comprehensive performance of sample 2 and sample 4 are larger than other samples. This means that the perforation indeed optimizes and enhances the comprehensive performance of the wavy fin heat exchanger, and with the increase of *Re*, the perforation enhances the comprehensive performance of the wavy fin heat exchanger more obviously.

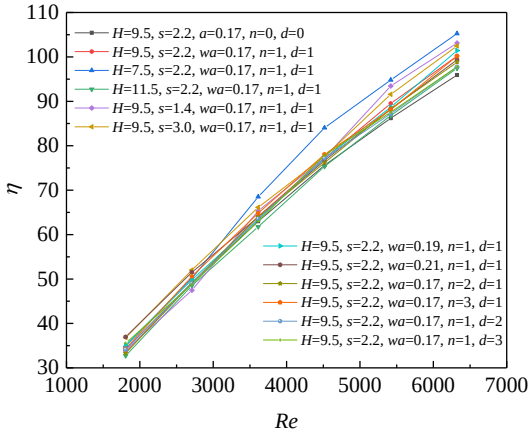

Fig.14 Performance factor η with *Re*

6. Conclusions

In this paper, the heat transfer and flow characteristics of perforated and unperforated wavy fins are investigated through experiments and numerical simulations. The influence of perforated wavy fin parameters (fin height *H*; fin pitch *s*; wave amplitude *wa*; perforation number *n*; perforation diameter *d*) on *Nu* and *f* is discussed. The main conclusions of this study are as follows:

(1) According to the experimental data, as *Re* increases, *Nu* increases while *f* decreases. With a constant *Re*, the *Nu* and *f* of perforated wavy fins are larger than those of unperforated wavy fins. The η shows that the comprehensive performance of the perforated wavy fin is significantly increased under high *Re*, and the performance of sample 2 is the best.

(2) The temperature field of the two wavy fins shows that the channel center temperature of the unperforated wavy fin is lower, and the variation is small, while the circular hole in the middle of the perforated fin destroys the thermal boundary layer and enhances the degree of air agitation, which is more conducive to the fin and air Heat transfer, the temperature in the center of the channel is higher.

(3) The numerical results show that under constant *Re*, both *f* and *Nu* increase with the increase of perforation diameter, wave amplitude, fin pitch and number of perforations. When *Re* is constant, *f* and *Nu* decrease as the height of the fin increases. In addition, as *Re* increases, *f* decreases, but *Nu* increases.

Acknowledgment

This research was supported by the School-enterprise Cooperation Project of Taicang Biaopu Technical Information Consulting Co., Ltd.(2020XQHZ05).

References

[1] Xu, G., *et al.*, Techno-economic analysis and optimization of the heat recovery of utility boiler flue gas, *Applied Energy*, *112*. (2013), dec., pp. 907-917

[2] Lee, C.-L.,C.-J.G. Jou, Saving fuel consumption and reducing pollution emissions for industrial furnace, *Fuel Processing Technology*, *92*. (2011), 12, pp. 2335-2340, DOI No. 10.1016/j.fuproc.2011.08.005

[3] Zhang, J., *et al.*, Generalized predictive control applied in waste heat recovery power plants, *Applied Energy*, *102*. (2013), FEB., pp. 320-326

[4] Jun, Y., Energy status and development trends of industrial furnace, *Energy for Metallurgical Industry*. (2011),

[5] Karthik, P., *et al.*, EXPERIMENTAL AND NUMERICAL INVESTIGATION OF A LOUVERED FIN AND ELLIPTICAL TUBE COMPACT HEAT EXCHANGER, *Thermal Science*, *19*. (2015), 2, pp. 679-692, DOI No. 10.2298/tsci120220146p

[6] Li, K., *et al.*, Multi-parameter optimization of serrated fins in PFHE based on fluid-structure interaction, *Applied Thermal Engineering*, *176*. (2020), p. 10, DOI No. 10.1016/j.applthermaleng.2020.115357

[7] Khoshvaght-Aliabadi, M., *et al.*, Role of channel shape on performance of PFHEs: Experimental assessment, *International Journal of Thermal Sciences*, *79*. (2014), 5, pp. 183–193

[8] Karthik, P., *et al.*, EXPERIMENTAL AND NUMERICAL INVESTIGATION OF A LOUVERED FIN AND ELLIPTICAL TUBE COMPACT HEAT EXCHANGER, *Thermal Science*, *19*. (2015), 2, pp. 679-692, DOI No. 10.2298/tsci120220146p

[9] Khoshvaght-Aliabadi, M., *et al.*, Effects of delta winglets on performance of wavy plate-fin in PFHEs Nanofluid as heat transfer media, *Journal of Thermal Analysis and Calorimetry*, *131*. (2018), 2, pp. 1625-1640, DOI No. 10.1007/s10973-017-6527-6

[10] Wen, J., *et al.*, Optimization investigation on configuration parameters of sine wavy fin in PFHE based on fluid structure interaction analysis, *International Journal of Heat and Mass Transfer*, *131*. (2019), pp. 385-402, DOI No. 10.1016/j.ijheatmasstransfer.2018.11.023

[11] Haider, P., *et al.*, A Transient Three-Dimensional Model for Thermo-Fluid Simulation of Cryogenic PFHEs, *Applied Thermal Engineering*. (2020), p. 115791

[12] Reneaume, J.M.,N. Niclout, MINLP optimization of Plate Fin Heat Exchangers, *Chemical and Biochemical Engineering Quarterly*, *17*. (2003), 1, pp. 65-76

[13] Reneaume, J.M., *et al.*, Optimization of Plate Fin Heat Exchangers:A Continuous Formulation, *Chemical Engineering Research & Design*, *78*. (2000), 6, pp. 849-859

[14] Picon-Nunez, M., *et al.*, Surface selection and design of PFHEs, *Applied Thermal Engineering*, *19*. (1999), 9, pp. 917-931, DOI No. 10.1016/s1359-4311(98)00098-2

[15] Mishra, M.,P.K. Das, Thermoeconomic design-optimisation of crossflow PFHE using Genetic Algorithm, *International Journal of Exergy*, *6*. (2009), 6, pp. 837-852

[16] Peng, H.,X. Ling, Optimal design approach for the PFHEs using neural networks cooperated with genetic algorithms, *Applied Thermal Engineering*, *28*. (2008), 5-6, pp. 642-650

Submitted: 9.3.2021.
Revised: 21.6.2021.
Accepted: 28.6.2021.